UCPH NanoScience
NanoVidenskab KU

tidsskrift.dk/index.php/NanoVidenskabKU

Thesis Paper

Platinum nanoparticles in photothermal therapy of cancer cells

Dunya Sarmad Aswad and Iliriana Qoqaj

Received June 2017, Accepted April 2018

Noble nanoparticles are potential photothermal therapy agents, due to their properties, such as ability to modify particle surface chemistry, and efficient light-to-heat conversion. In this work, we study the possible application of platinum nanoparticles as agents in photothermal therapy, their uptake, and toxicological response in the human ovarian cancer cell line (SK-OV-3) by flow cytometry. No oxidative stress, or toxicological response of the platinum nanoparticles was observed in the cells. Laser irradiation revealed photothermal destruction of SK-OV-3 cells exposed to 70 nm platinum nanoparticles at power density 45 W/cm^2 after 5 minutes using an 808 near infrared laser.

Introduction

Nanotechnology has offered a revolutionary breakthrough throughout the past years in the fight against cancer[1,2]. It has created new methods for cancer diagnostics, drug delivery and therapeutics[3]. Currently, different approaches are used to treat cancer, the most common being chemotherapy and radiation therapy, but these are not the most optimal methods, as they also attack healthy cells in the body in addition to the cancerous ones. By scaling down materials to nanometer scale we find nanoparticles (NPs) with extraordinary properties, including optical, magnetic, electronic and structural properties, which makes these nano-scaled particles promising for different approaches in the biomedical field[3,4]. Gold nanoshells (Au NSs), consisting of a silica core surrounded by a gold shell, have received much attention because of their excellent properties, such as their surface modification, biocompatibility, and efficient light-to-heat conversion[4–6]. Previous studies have shown that Au NSs could be the most promising NPs so far[5,7]. The potential difference that could separate treatment with NPs from chemotherapy and radiation therapy could be that the amount of healthy cells being attacked would potentially be reduced as well as the amount of cancer cells that die would be increased[1,3]. Plasmonic noble metal NPs have long been researched, due to their remarkable surface plasmon resonance (SPR)[4,8]. When metal particles are exposed to light, it induces an oscillation of the free electrons of the metal[4]. The SPR happens when the amplitude of the oscillation reaches its maximum at a specific frequency[4]. The SPR produces a strong absorption of the light and that absorption can be measured using a UV-Vis-NIR spectrometer[4]. The wavelength where the absorption peaks, is where the particles gets heated up most efficiently. This resonance peak also acts as a marker of the most effective laser wavelength to use for treatment[4]. A spectrometer is an instrument in which the reflection and absorption characteristics of a sample is measured, termed absorbance[9]. The radiation wavelength for the ultraviolet (UV), visible (vis), and near infrared (NIR) regions can be defined from 300 nm to 400 nm, 400 to 765 nm, and 765 nm to 3200 nm, respectively[10]. The absorbance can be used to characterize the optical properties of NPs. To determine some of the properties of NPs (or other macromolecules), including their size and shape, the common technique, dynamic light scattering (DLS) can be used[11–13]. The first outcome from a DLS experiment is an intensity distribution of the particle sizes[13]. Particles experience Brownian motions when suspended in liquid, and random collisions with solvent molecules causes particles to diffuse throughout the liquid[13]. The particles are irradiated with a laser, and the light is scattered. The observed intensities of the scattered light are the result of the interference of light scattered by each particle, which depends on the position of each element, this is known as the diffusion coefficient[13].

In recent years, scientists have been curious about the general properties of Pt NPs[14,15]. Our interest for Pt NPs are their possible application in the particle enhanced photothermal treatment (PTT) of cancer tumours. PTT relies on NPs with high light absorbing properties that are taken up by cancer cells. NPs get irradiated by a laser with wavelength in the NIR region and transform the light into localized heat energy, that penetrates the tissue, melts the lipids and kill targeted cell, hopefully, without damaging non-targeted cells[3,16,17]. The advantage of the NIR wavelength region is due to the biological window or therapeutic window, which is a range of wavelengths where light has maximum depth of penetration in tissue and low absorption[5,7]. Heating of the NPs leads them to oscillate, possibly causing the cancer cells to die either from active self-destruction (apoptosis) or from swelling until they burst (necrosis), tumour growth is stopped and the cancer cells are destroyed[18]. PTT is a well-researched topic as it could possibly replace methods being used at the present[3,7,18,19].

Cell death can occur in different situations, for example by apoptosis or necrosis. Apoptosis are recognized as the most common type of “programmed” death that occurs, especially during embryonic development[20,21]. Apoptosis can also occur as defence mechanism when cells are damaged by several causes.

Phosphatidylserine (PS) is a phospholipid, preferably located on the cytosolic portion of the plasma membrane, in normal viable cells (normal conditions)[21]. While, during apoptotic conditions a systematic change occurs in the plasma membrane as a result from the apoptotic signal. PSs are translocated from the cytosolic portion (inner leaflet) to the outer section (outer leaflet) of the plasma membrane, which exposes the PSs to the outside cellular environment[22–24]. The human vascular anticoagulant, Annexin V, is a protein that is commonly used as a bait to examine cells that are apoptotic, as Annexin V is a Ca^{2+}- dependent phospholipid- binding protein that binds to PS[21,24]. Annexin V tends to attach to phospholipids (phospholipids are the integral part of the cell membranes)[21]. In the early stage of apoptosis, once the cell is transferred to the apoptotic condition, Annexin V will bind to the PSs in the presence of Ca^{2+} and this can be detected by adding a fluorescence tag to Annexin V. Annexin V can therefore act as an apoptotic assay[24]. Necrosis is an accidental and inactive kind of cell death induced from environmental changes and is normally considered to be an uncontrolled kind of cell death[22,25,26]. Necrosis is often referred to as a kind of damage that happens spontaneously, although it can be classified as programmed cell death in some situations[27]. Necrosis occurs mostly when the cell swells up and the membrane then collapses leaving the cell destroyed[27]. The LIVE/DEAD stain can be used to examine the viability of cells by flow cytometry[28]. Necrotic cells have permeable cell membranes which can results in intense fluorescent staining as the dye will stain the whole cell due to the reaction of the amines in the cell[28]. Whilst, living cells will show a weak fluorescent staining as the dye only react with the amines on the cell surface. This approach can be used to investigate whether the cells die when exposed to NPs[28,29]. Oxidative stress, refers to the "raised intracellular levels of reactive oxygen species (ROS)"[30] that can cause damage to DNA, protein and lipids. ROS are chemically reactive molecules containing oxygen. If oxygen gains one or two electrons, it can lead to the formation of molecules such as superoxides or peroxides that can potentially be dangerous to the cells. These and other dangerous oxygen derivatives are called ROS[30]. If these ROS produces are not actually controlled, they can react with cell components and cause oxidative damage, among other things, cancer[30]. These ROS has two faces – redox biology, which occurs in the body all the time, where a small increase in ROS concentration activates biological processes[30]. Whilst, oxidative stress designates high concentrations of ROS which leads to damage of DNA, proteins and lipids[30]. Meaning that large changes are usually an indication of oxidative stress causing toxicity[30]. NPs can be toxic to the cells and sometimes the cells undergo oxidative stress because of the NPs toxicology and produce these ROS, which is a form of stress marker[31,32]. CellROX Oxidative Stress Reagents (Deep Red) are fluorescent probes that have the feature to detect and measure reactive oxygen species (ROS) in living cells. The fluorescence resulting from CellROX Oxidative Stress Reagents can be measured by using flow cytometry[31]. Cell analysis can be performed by a flow cytometer where thousands of cells pass through a laser beam per second and capture the light signal from each cell as it passes through[33,34]. The data gathered can be analysed statistically by a flow cytometry software to report cellular characteristics such as size, complexity, phenotype and health[33–35]. The interrogation point is the center of the system. This is where the laser and the sample criss-cross and the optics collect the resulting scatter and fluorescence[34,35]. Laser light is used to detect individual cells in the stream, as a cell passes though the laser it will refract or scatter light at all angles[33,34]. Fluorescence gives information about structure and function of cells, the fluorescent signal is emitted and detected[33,34]. Forward scatter (FSC) is when light is refracted by a cell in the flow channel and continues in the direction of the light travelling path (light scattered in the forward direction). The refracted light is detected by a detector. The magnitude of FSC is roughly proportional to the relative size of the cell. Therefore, generally smaller cells will produce smaller amount of forward scattered light and larger cells will produces larger FSC[34]. Side scatter (SSC), on the contrary, to forward scattered light, the light is scattered in a direction outside the light travelling path. This scattered light is focused through a lens system and is collected by a separate detector usually located perpendicular from the lasers path, these detectors usually gives information about the cell granularity and complexity, and in some cases how many NPs are present in the cell[33,34]. Therefore, cells with large complexity and high granularity produce more scattered light, than a cell with low complexity and low granularity[34]. Increase in SSC signal in cells have been associated with increasing NP uptake[8].

The aim of this study is the possible application of Pt NPs in PTT of a cancer cell model. We investigated if Pt NPs with diameters of 30 nm (Pt30), 50 nm (Pt50) and 70 nm (Pt70) were taken up by cells (by SSC detection using flow cytometry). In this study we used a human ovarian cancer cell line (SK-OV-3), that overexpresses the HER-2 (Neu/ErbB-2) gene[29], which is a tyrosine-protein receptor that is highly expressed in some cancerous cells[29,36]. To characterize the optical properties, we want to perform UV-Vis analysis, and to investigate if different medium conditions change the hydrodynamic size, we will perform DLS analysis. Furthermore, we will examine if the Pt NP uptake leads to a toxicological response in the SK-OV-3 cells by them self (with no laser treatment), as some noble metals have revealed being toxic[37–39]. Moreover, we will examine the stress level (if any) the Pt NPs induce in SK-OV-3 cells, with the use of CellROX.

Methods

Particle characteristics by manufacturer

The Pt NPs were declared to be spherical and citrate stabilised by manufacturer. The characteristics of the Pt NPs declared by the manufacturer (nanoComposix) are listed below.

Table 1 *Characteristics of the different sized platinum nano-particles (Pt NPs) declared by the manufacturer.*

Pt NPs	Diameter (TEM)	Coefficient of Variation	Hydrodynamic Diameter
Pt30	30 ± 3 nm	11.2 %	39 nm
Pt50	51 ± 7 nm	13.2 %	61 nm
Pt70	71 ± 4 nm	5.1 %	71 nm

Cell culture

Human ovarian cancer (SK-OV-3) were grown in cell culture flask using McCoy's 5A medium (GE Healthcare Life Sciences, HyClone Laboratories) under normal cell growth conditions at 37℃, 5% CO_2 and 95% humidity.

Cells for experiments were seeded in 24-well cell culture plates (Nunclon Delta, Nunc, Thermo Fischer Scientific) or 35 mm petri dish with, 20 mm microwell (Part No# P35G-1,5-20-C, MatTek Corporation) in McCoy's 5A growth medium with a seeding density of 2.5 x 10^4 cells per cm^2 under normal cell growth conditions at 37℃, 5% CO_2 and 95% humidity. The cells were count by using a cell counter (Countess II FL, life technologies).

Nanoparticle preparation and cellular exposure

The nanoparticles were prepared by centrifugation (Eppendorf, Centrifuge 5417C) and removing of supernatant and then sonicated for 5 minutes (2510 Brandson). Then the particles were re-suspended in the relevant solution. For cell exposure, UV-Vis and DLS, McCoy's 5A medium (with no phenol red) with 10% foetal bovine serum (FBS) was used, Milli-Q water (18.2 MΩ at 25℃, Ultrapure (Type 1) Water, Direct-Q*3 UV) were used for UV-Vis and DLS experiments.

For cell exposure experiments, normal McCoy's 5A medium was removed and replaced with NP containing McCoy's 5A medium one day after seeding, and was added at the described concentrations. The cells were incubated for 24 hours under normal cell growth conditions.

Nanoparticle characterisation

The optical properties of the NPs were examined by UV-Vis *(See Appendix, Figure 1-4)* (Agilent Technologies, Cary 5000 UV-Vis-NIR Spectrophotometer), and the hydrodynamic sizes were examined by DLS (Malvern Instruments Nordic) done by placing a small sample of the solution we want to investigate in the machine using a cuvette.

The experiments were performed for particles in the following conditions: in Milli-Q water, McCoy's 5A medium after 0 hour of incubation, McCoy's 5A medium after 24 hours incubations (37℃), and McCoy's 5A medium after 24 hours incubation together with cells (under normal cell growth conditions).

Flow cytometry and sample preparations

For flow cytometry experiments cells were seeded in 24-wells and exposed to Pt NPs as previously explained.

CellROX medium was prepared by adding CellROX® Deep Red (#cat C10422, Molecular Probes) in McCoy's 5A medium for each sample and it was protected from light.

The 24-well containing cells was placed on a cooling block. The cells were transferred to Falcon FACS tubes (Falcon®), and the well was washed with ice-cold Annexin V binding buffer (aVbb) and placed on a pre-cooled cooling rack. The cells were centrifuged for 5 min at 400 x G, and the supernatant were removed and the cells were re-suspended in aVbb with LIVE/DEAD® Fixable Near-IR Dead Cell Stain (LD) (cat# L34975, Molecular Probes) diluted 1:1000 from stock solution. Annexin V alexa488 V Alexa Fluor® 488 (cat# A13201, Molecular Probes) diluted 1:100 from stock solution (concentration was not mentioned) were added to each sample, and were incubated for 30 minutes protected from light. Ice-cold aVbb was added to each sample, and the cells were centrifuged for 5 minutes at 400 x G, the supernatant was then removed. Finally, ice-cold aVbb was added and the samples were kept on ice until analysis on the Flow cytometer.

Control samples with no Pt NPs and staining was also prepared, as well as single staining controls for each probe (CellROX, Annexin V, and LD). These controls were used to perform digital signal compensation to remove overlapping fluorescent signals (spectral mixing) between the different fluorophores.

Cell damage were examined by flow cytometry. Cell death assay were performed using Flowing Software (version 2.5.1). This assay gives an idea of the state the cells are in and if they react to the particles. We placed a quadrant on the dot plot and thus the cells can be divided into living cells (lower left) with a low Annexin V and LD signal, early apoptotic cells (upper left) with a high Annexin V and low LD signal, late apoptotic (upper right) with a high Annexin V and high LD signal, and necrotic cells (lower right) with a low Annexin V high LD signal. *(See Appendix for illustration, figure 5 and 6)*

Flow cytometry was performed on a BD FACS canto II (Becton, Dickinson and Company). FSC and SSC were detected using blue laser (488 nm) and detection at the same wavelength. The levels of Annexin V, Alexa Fluor® 488 conjugate was detected using blue excitation laser (488 nm) and a 530/30 nm emission filter. CellROX® Deep Red Reagent and LIVE/DEAD® Fixable Near-IR Dead Cell Stain was detected using red excitation laser (633 nm) and a 660/20 nm emission filter and a 780/60 nm emission filter, respectively.

Laser exposure and imaging

Cells were seeded on 35 mm petri dish with, 20 mm microwell. 24 hours after exposure to Pt NPs (or 24 hours after cells seeding for laser treatment only) the Pt NP exposure medium was removed and cells were washed 3 times with PBS, and replaced by McCoy's 5A medium (without phenol red). Laser treatment was performed by a Modulight ML6600 laser system (Modulight) using a custom 5 mm spot illumination kit.

24 hours after the laser treatment the cell medium was removed and replaced with cell medium containing 5 µM calcein-acetoxymethyl (AM) (Molecular Probes), "a membrane-permeable live-cell labeling dye" a probe that only fluoresces in live cells, and cells were incubated for 15 min. Cells were imaged using cell medium without phenol red.

Cells were imaged using the Nikon wide-field fluorescent microscope (Eclipse T*i*) using the FITC excitation/emission cube set. *(See Appendix for detailed protocols, page 4-6).*

Statistics

All statistical test was performed using IBM SPPS statistics (version 24). ANOVA was performed, and to test for homogeneity of variance Levene's test was performed. For data passing Levene's test of similar variance between groups, a Tukey post-hoc test was performed, for samples failing Levene's test a Gemes-Howell post-hoc test was used. In all cases a significant level of $P < 0.05$ was used. *(See Appendix for further details, page 7-16).*

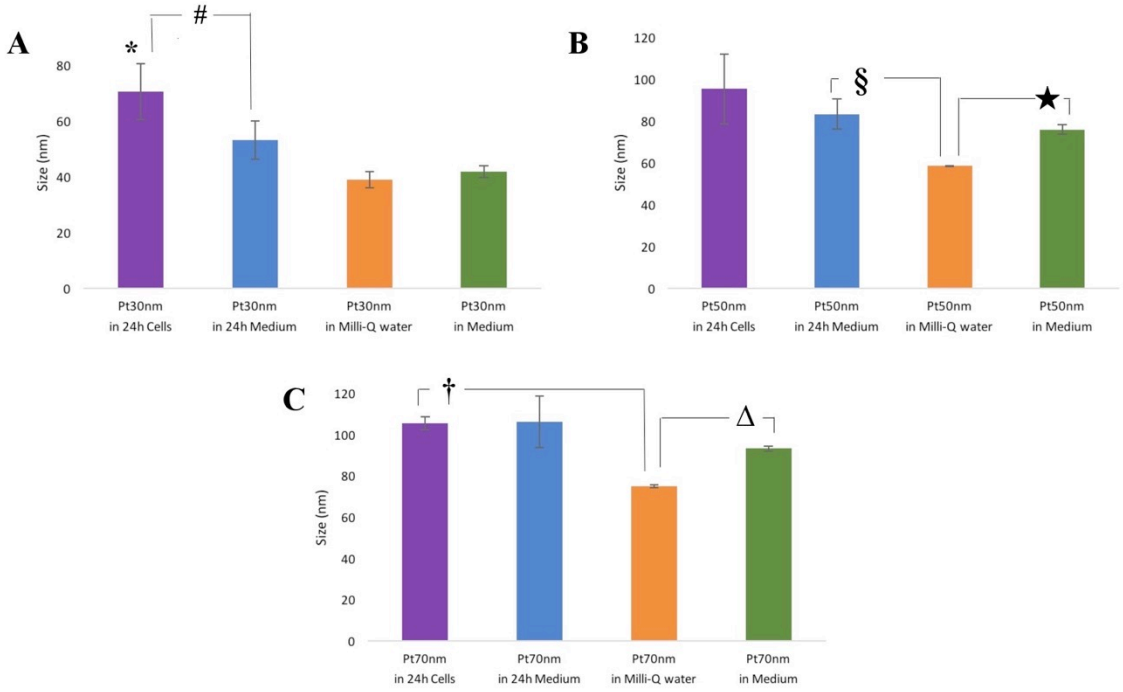

Figure 1 *Dynamic light scatter (DLS) analysis of platinum nanoparticles (Pt NPs) with a diameter of 30 nm, 50 nm, and 70 nm, respectively. Panel **A** shows the mean hydrodynamic size of Pt30 in different conditions, with cells for 24 hours (purple), in medium for 24 hours (blue), in MilliQ water (orange), and in medium (green). # P = 0.094 and * P < 0.005. In the same conditions is also shown for Pt50 (Panel **B**) § P = 0.096 and ★ P = 0.023, and for Pt70 (Panel **C**) † P = 0.009 and Δ P = 0.000.*

Results

Nanoparticle characterisation

We determined the hydrodynamic sizes of the different Pt NPs by DLS *(Figure 1)*. In Milli-Q water the Pt30 showed a small increase in size with an average of 38.9 nm and a standard deviation of 2.89. The Pt50 showed a small increase as well with an average of 58.5 nm and a standard deviation of 0.22. Finally, the Pt70 also showed the same increase with an average of 74.8 nm and a standard deviation of 0.74.

In medium the Pt NPs showed a consistent increase of the diameter between 10-30 nm *(Figure 1)* compared to Milli-Q water.

The Pt NPs were also investigated after a 24-hour period in medium which showed a 20-40 nm increase of the diameter *(Figure 1)*. Furthermore, the PtNPs were investigated over a 24-hour period incubated with SK-OV-3 cells. Characterization showed that they all increased approximately 40 nm in average diameter *(Figure 1),*

In *Figure 1, Panel **A*** we observed a significant increase of Pt30 in 24 hours cells. It is significantly different from Milli-Q water (P = 0.005) and medium (P = 0.008). The interest is whether there is a difference between the diameter of the NPs when in 24 hours cells, and 24 hours medium. It appears that they are slightly larger, when in 24 hours cells, but it is not significant, however close, due to the low P-value (P = 0.094).

From the statistics, in *Panel **B** (Figure 1)* Pt50 showed a significant difference in medium (P = 0.023) compared to Milli-Q water. The Pt50 in 24 hours medium, showed being close to significant (P = 0.096) also compared to Milli-Q water.

Finally, in *Panel **C** (Figure 1)*, Pt70 in 24 hours cells showed to be significantly different from Milli-Q water (P = 0.009) and medium is significantly different from Milli-Q water as well (P = 0.000).

The Poly Dispersity Index (PDI) is a width parameter that gives information about the dispersity of the sizes *(Table 2)*.

From the statistical interpretation, we observed that Pt30 in Milli-Q water was significantly different to all conditions with a P value of 0.000. Pt50 in Milli-Q water showed a significant difference from medium (P = 0.000), and 24 hours medium (P = 0.029). Pt70 in Milli-Q water showed a significant difference from medium (P = 000.0) and also 24 hours medium (P = 0.001).

Table 2 *Dynamic light scattering (DLS) analysis of the different sized platinum nanoparticles (Pt NPs). The mean values of the Poly Dispersity Index (PDI) indicates the spread in the distribution of the Pt NP sizes in the different conditions.*

Pt NPs	**Solutions**			
	24h Cells (PDI)	**24h Medium (PDI)**	**Milli-Q water (PDI)**	**Medium (PDI)**
Pt30	0.52±0.02	0.51±0.01	0.23±0.04	0.5±0.002
Pt50	0.35±0.08	0.29±0.02	0.14±0.002	0.27±0.004
Pt70	0.32±0.11	0.23±0.01	0.08±0.008	0.21±0.007

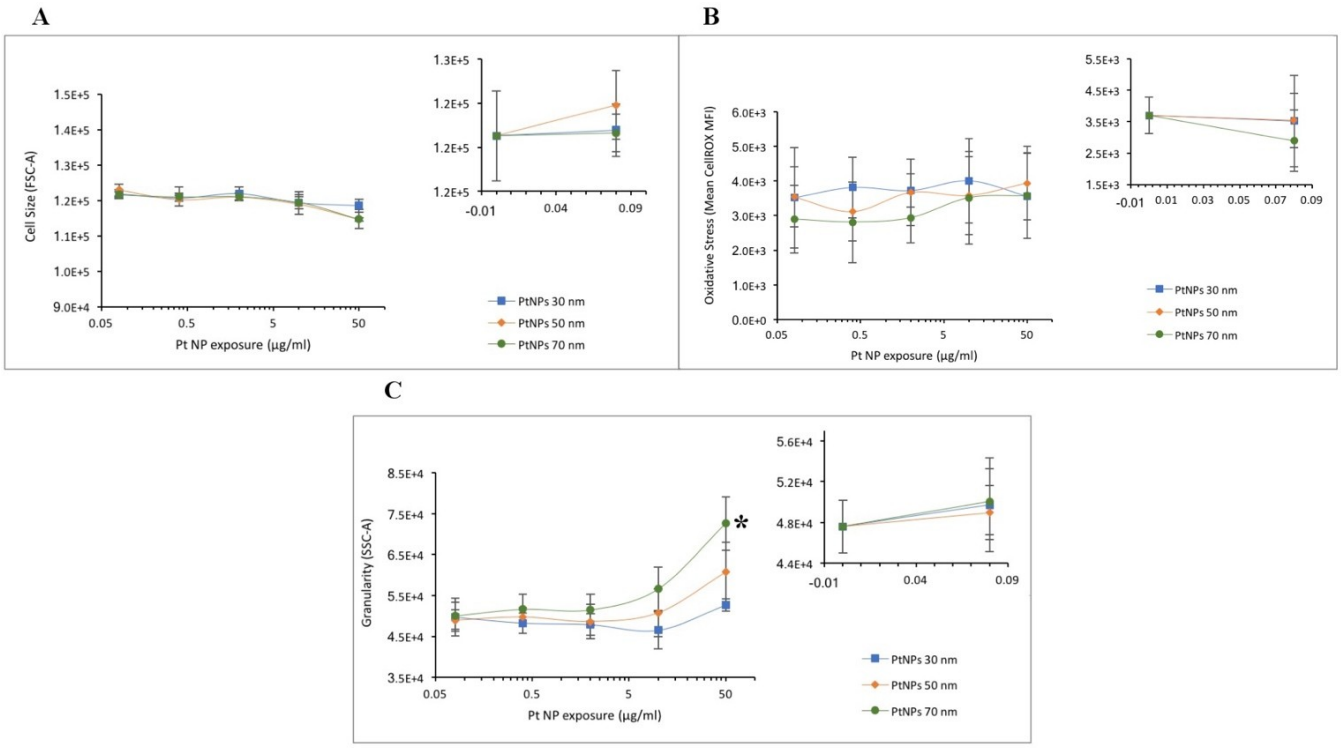

Figure 2 *Flow cytometric analysis of SK-OV-3 cells in different concentrations of platinum nanoparticles (Pt NPs). Panel* ***A*** *shows the size (FSC-A) of cells exposed to particles at different concentrations, 0.08, 0.4, 2, 10, 50 µg/ml. The window illustrates the SK-OV-3 cells with no particles and with 0.08 µg/ml. Panel* ***B*** *shows oxidative stress (CellROX) of cells exposed to particles at different concentrations, 0.08, 0.4, 2, 10, 50 µg/ml. The window illustrates the SK-OV-3 cells with no particles and with 0.08 µg/ml. Panel* ***C*** *shows the granularity (SSC-A) of cells exposed to particles at different concentrations, 0.08, 0.4, 2, 10, 50 µg/ml. The window illustrates the SK-OV-3 cells with no particles and with 0.08 µg/ml. * P < 0.000.*

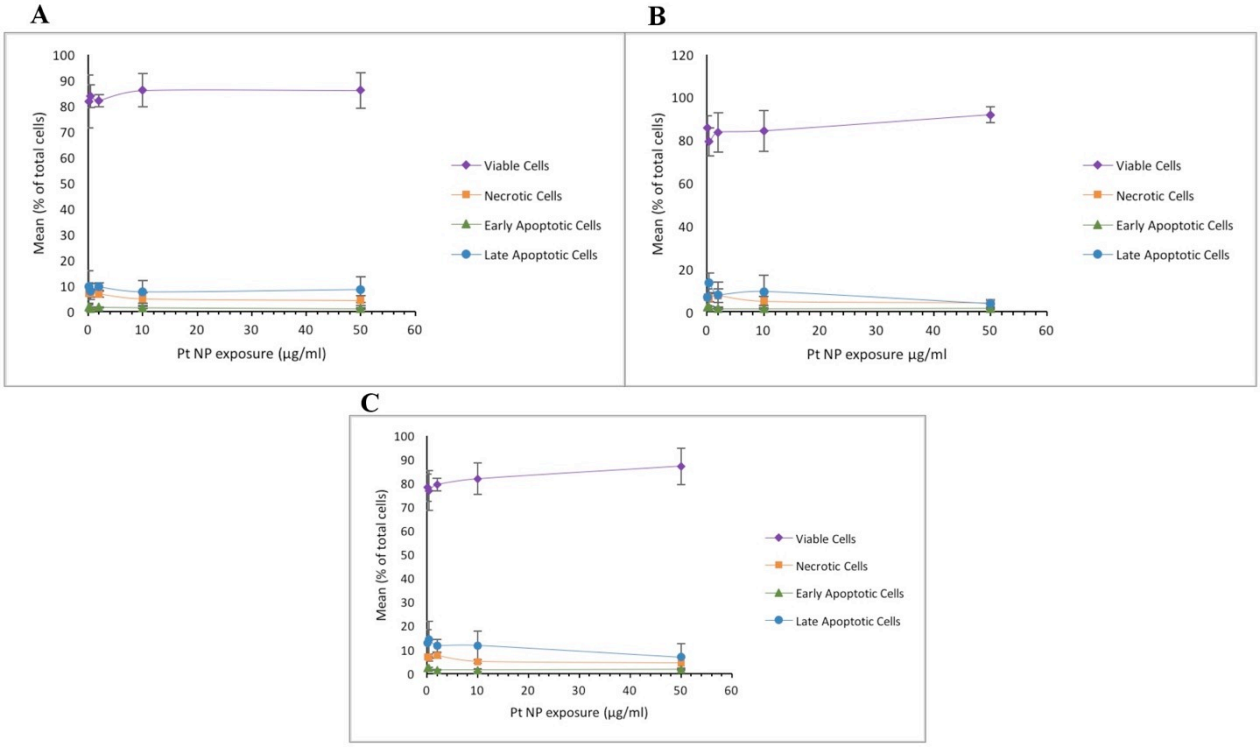

Figure 3 *Flow cytometric analysis of SK-OV-3 cells treated with Annexin V (Alexa Fluor 488®) and LIVE/DEAD™ stain. Cell death assay show the living and dead cells, respectively. The dead cells are divided into early apoptotic, late apoptotic, and necrotic. This applied when the cells were exposed to Pt30 (Panel* ***A****), Pt50 (Panel* ***B****), and finally Pt70 (Panel* ***C****).*

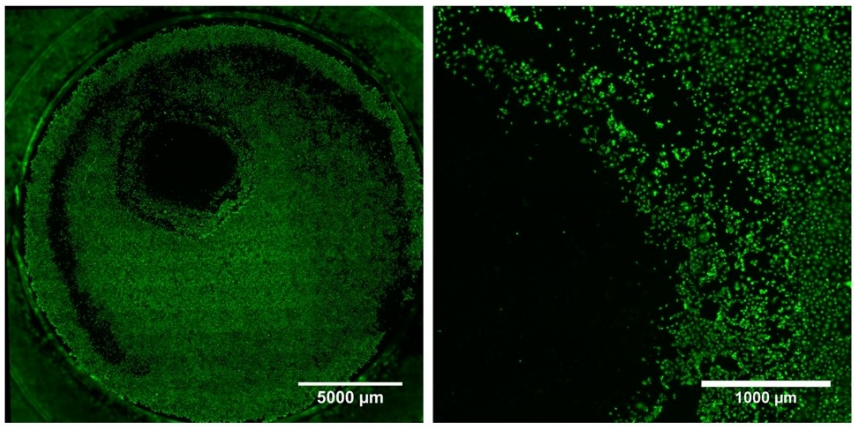

Figure 4 *Microscope images after laser treatment (808 nm, 45 W/cm^2, 5 min) of SK-OV-3 cells with Pt70 NPs.*

Measurement of PtNP-uptake, oxidative stress and cell death by flow cytometry

The SK-OV-3 cells were exposed to a concentration of 0-50 µg/ml of Pt30, Pt50, Pt70 for 24 hours *(Figure 2, panel **C**)*. We did not observe any significant increase of the cell granularity (SSC-A) before 10 µg/ml, for all Pt NP size. Only at 50 µg/ml we observed a significantly increase in granularity for cells exposed of 70 nm Pt NPs ($P < 0.000$). In comparison, there was not observed any significant change in cell size (FSC-A) for cells exposed and unexposed to Pt NPs *(Figure 2, panel **A**)*.

The CellROX measurement *(Figure 2, panel **B**)*, did not show any sign of oxidative stress in the cells when exposed to different concentrations (0, 0.08, 0.4, 2, 10, 50 µg/ml) of Pt NPs. The values were consistent which the statistical interpretation also indicates, no significant level of $P < 0.05$.

In the cell death assay *(Figure 3)*, there was no observed difference of all the parameters, viable cells, necrotic cells, early apoptotic cells, and late apoptotic cells. For cells after 24 hour exposure to all concentration of Pt30, Pt50, and Pt70, relative to cells not exposed to NPs. This was also observed in the statistical interpretation.

Laser treatment and microscopy image

The laser treatment analysis discloses that SK-OV-3 cells exposed to Pt NPs are demolished (killed) after five minutes of the laser treatment at 45W/cm^2 using an 808 nm laser. The laser power indicates how much energy is transferred to the cells. Observing the laser treatment with Pt NPs, cell death is observed – while the control sample, with cells and laser only, there is no observed cell death. Furthermore, the exposed laser area in the well showed a clear damage of the cells, this implies a high localized photothermal effect.

The controls without Pt NPs showed no cell damage after laser exposure, at different laser power densities from 5 to 45 W/cm^2. *(See Appendix, figure 7)*

The dark spot indicates photothermal destruction induced by Pt NPs. It can be verified that the cells died as a result of the laser radiation as the dark spot is measured to be 5000 µm, and the laser produces a homogenous 5 mm diameter beam, according to the laser manufacturer.

The laser treatment was repeated with all sizes of Pt NPs, but no photothermal effect was observed. This could either be due to a problem with particle exposure or the laser itself. The reason for the failed photothermal effect is still ongoing.

Discussion

The DLS data showed a pattern as all the hydrodynamic sizes increased from what the manufacturer stated. In Milli-Q water they are a lot smaller and so is the standard deviation, in comparison to when the Pt NPs are in 0 hour medium, 24 hours medium or 24 hours cell medium. When NPs are in biological fluid they associate with proteins[40]. The proteins adsorb to the surface of NPs, resulting in forming a protein layer around the NPs, this is termed the protein corona[41]. Other studies have also observed an increase in the hydrodynamic size of Au NPs due to a possible protein corona formation on the NP surface[8,12,42]. The formation of the protein corona is determined by factors as the NP surface chemistry, size, and charge[41]. The protein coronas compositions and molecular properties have shown to be important factors of the cellular uptake of NPs[41]. The fully interactions between NPs and proteins are yet to be further studied[40,41]. The results from flow cytometry, showed a concentration-dependent relationship between the exposure and cellular Pt NP-uptake in the SK-OV-3 cells for high concentrations of Pt NPs. Klingberg *et al.,*[8] had similar observations of a concentration-dependent increase in granularity[8]. The increase in the granularity indicates that there is an uptake of these particles by the cells, due to a greater reflection of increased complexity of the cells. It is easiest to see the uptake of the Pt70, as it is most significant. We cannot conclude from this, that Pt70 has the best uptake in the cells, this can be further examined by ICP-MS, as other studies have for other noble NPs[8,43]. The toxicity of NPs is an important concern, as it is crucial for the use in PTT. The effects of NPs on cellular health depends on the NPs size, shape and surface change[44]. Silver is referred to as the toxic NP[14,37–39], which is why we investigated if Pt NPs showed a toxicological response. The most researched NP are the Au NPs, they have been researched in various different sizes and shapes.

Some experimental works confirms that Au NPs are not toxic[44–46] yet other experiments and investigations revealed a toxicity of the particles[44,47,48]. Gold nanorods have been found to be toxic, however that is due to the synthesis of the rods, as they are usually stabilized in the surfactant cetyltrimethylammonium bromide (CTAB), unlike gold and Pt NPs that are usually stabilized with small molecules such as citrate. An interesting paper by Takahashi *et al.,*[49] investigated the cytotoxicity of gold nanorods to a human epitheloid cervix carcinoma (HeLa) cell line where they substituted the CTAB solution with phosphatidylcholine (PC) and the results showed a low cytotoxicity compared to the gold nanorods stabilized with CTAB[44,49].

We performed a cell death assay[34] to investigate whether the Pt NPs were toxic to SK-OV-3 cells. The assay did not show any difference in cell death due to exposure to particles. Even at high concentrations of Pt NPs, there were no difference in the amount of dead cells. This is an optimistic result as it confirms that the particles were not toxic to the cells. In comparison to our experiment, Villiers *et al.,*[44,50] investigated Au NPs incubated in dendritic cells, they found a non-toxic response of the Au NPs in the cells, even at high concentrations.

Oxidative stress in the cells were also examined and did not show any significant difference within the used concentrations when the particles were added to the cells, indicating no evidence of induced oxidative stress. From these experiments, we assume that the particles are not toxic for SK-OV-3 cells. Since there are no changes in cell death and oxidative stress despite the relatively high concentrations of particles, we would expect that the cells will not be damaged by the exposure of Pt NPs, and we will thus be able to continue with the cell experiments without worrying about inducing a toxicological effect with the particles alone.

In a work from Tedesco *et al.,*[51] they examined oxidative stress and cytotoxicity of Au NPs with a diameter of 5.3 nm, and their results showed that the small sized Au NPs caused oxidative stress and cytotoxicity significantly more, than other studies have for Au NPs of larger sizes[47,51]. This could give rise to think whether our experiment could have shown if the use of smaller Pt NPs sizes would have induced oxidative stress and toxicity, but we did not observe this for Pt30 compared to Pt50 or Pt70.

PTT has been proved to be an effective weapon against different cancer models. Nanoparticles in collaboration with the NIR laser have repeatedly managed to kill cancer cells[16,52,53].

Numerous studies, have experimented with different NPs, wavelengths and power densities. These studies all have in common that they succeed to kill the irradiated cells with NPs. El-Sayed *et al.,*[54] demonstrated the efficiency of gold nanospheres as a photothermal agent in vitro to two oral squamous carcinoma cells (HOC and HSC) and one epithelial cell line (HaCaT) that overexpresses EGFR, a cancer biomarker. The laser used for their experiments operated at 514 nm, and the used power densities were 19, 25, 38, 50, 64, and 76 W/cm^2, respectively, to irradiate cells for 4 minutes. The cells were irradiated at a power density of 76 W/cm^2 in the absence of NPs, it was here observed that no cell death had occurred. They demonstrated that HaCaT cells after incubation with anti-EGPR antibody conjugated Au NPs showed the photothermal effect with the laser density of 57 W/cm^2 or above. The HSC cells showed cell death when exposed to a laser density of 25 W/cm^2, whilst at 19 W/cm^2 and lower laser densities, no cell death was observed. Laser treatment of HOC cells showed cell death at a much lower laser density at 19 W/cm^2, whilst at 13 W/cm^2 and lower laser densities, no cell death was observed. In conclusion, they state that for clinical application of cancer treatment on tissue, a NIR laser light is needed, preferably between 650 and 900 nm that can penetrate in larger depths[54]. Later El-Sayed *et al.,*[16] upgraded their experiments and worked with gold nanorods at higher wavelength due to the earlier mentioned biological window. They now operated at 800 nm. They irradiated the cells at different power densities for 4 minutes each. Their results showed that the HOC and HSC cells were injured at 10 W/cm^2. HaCaT cells were injured at 15 W/cm^2 and died when exposed to 20 W/cm^2 and above at 800 nm[16]. These results and findings indicate that there could be a correlation between the laser wavelength and power. Bernardi *et al.*[52] demonstrated the use of gold-silica nanoshells (immunonanoshells), their reasoning of using nanoshells is due to their extremely efficient absorption of NIR, and their great converting abilities to generate laser light into heat to kill cancer cells. In this study, they demonstrated the use of a laser at 800 nm and 80 W/cm^2 for 2 minutes in medulloblastoma cell line (Daoy.2)[52]. Their results describe that the strategy used can selectively kill cells that express the HER-2 gene without killing cells that do not express the gene. This is due to Bernardi *et al.,* modified the used gold-silica nanoshells to be incorporated into HER-2 positive cells (antibody), but they are not taken up by other cells due to polyethylene glycol (PEG)[52].

In El Sayed *et al.,*[54] study, we found that when using a laser at lower wavelength (514 nm), they used higher power densities for the HaCaT cells (57 W/cm^2), to observe destruction[54], whilst we observed destruction at laser density at 45 W/cm^2 for SK-OV-3 cells. Both in the presence of NPs. The other two cell lines they irradiated already showed cell death at 25 W/cm^2 and 19 W/cm^2. Comparing these results to the later study of El Sayed *et al.,*[16] where they used a higher laser wavelength (800 nm), here they observed cell death at lower power densities than in their previous study[54]. This could indicate that some cell lines are more susceptible to laser treatment and can thus be destroyed by lower laser power densities. In the absence of NPs our experiment did not show cell death at 45 W/cm^2 when using an 808 nm laser. El Sayed *et al.*,[54] made a similar control experiment without NPs in their cells, neither of them were injured even at a high power density (76 W/cm^2). These observations are surprisingly at these laser power densities compared to other studies with example SK-BR-3 cells and Au NSs (820 nm, 35 W/cm^2 for 7 min)[53]. Another interesting work of Van de Broek *et al.,*[29] where they used branched gold nanoparticles biofunctionalized with antibodies as potential photothermal therapy agents in SK-OV-3 cells, they observe cell destruction after laser treatment (690 nm) at 38 W/cm^2 for 5 minutes[29]. This observation by Van de Broek *et al.,* is in accordance with what we also observed for the same type of cells.

All these different studies, implies that the experiments also depend on the cell type, as some cells could be more resilient to treatment. They all have in common that they manage to induce a photothermal effect in different cell lines. PTT has many factors that take part in whether the experiment is successful or not, for

example the use of different laser wavelengths, power densities, cell lines and most importantly, the particles used in the experiment could give changes in the outcome.

In conclusion, our experiment and results showed that cellular uptake of the Pt NP was efficient. Furthermore, we observed that the Pt NP uptake did not lead to a toxicological response, and no level of stress was induced in the SK-OV-3 cells, at the given concentrations. Finally, the laser treatment with a wavelength of 808 nm at 45 W/cm^2 for 5 minutes, demonstrated that we were able to perform a photothermal effect in the SK-OV-3 cells in presence of 70 nm Pt NPs, whilst cells in the absence of Pt NPs were not harmed using the same laser treatment.

Further work

In further work, we could take advantage of SK-OV-3 cells that have a high surface expression of the protein HER-2, which is a protein found in certain forms of cancer. HER-2 is highly expressed in SK-OV-3 cells so it is easy to target them.
We chose a cell type that could be used in further work to make a regressive tumour model in nude mice.
The use of NPs for cancer treatment still has a lot of work ahead, and the investigation of whether cells die from the laser treatment or from the NPs, and in that case, which wavelength and power density are most ideal? The next step could be to further develop Pt NPs so they can work more efficiently and at lower dose.

Acknowledgements

Special thanks, to our supervisor Postdoc Henrik Klingberg, for supporting, helping and guiding us through this bachelor project over this period. We would also like to thank Associate Professor Poul Martin Bendix for introducing us to the Optical Tweezers Group, and Professor, PI of Optical Tweezers Group, Lene B. Oddershede for introducing us to the project.
This project was part of Laser activated nanoparticles for tumor elimination (LANTERN) funded by Novo Nordisk Foundation Interdisciplinary Synergy Programme. We would like to thank Professor Andreas Kjær, cluster for molecular imaging a LANTERN partner for the use the flow cytometer.
Lastly, we would like to thank all the group members of the Optical Tweezers Group for their welcomeness and company over this period.

Address: Nano-Science Center & XXXXXXXXX, University of Copenhagen, Universitetsparken 5, 2100 København Ø, Denmark.; E-mail: svg537@alumni.ku.dk and xnq328@alumni.ku.dk

References

1. Porcel, E. *et al.* Platinum nanoparticles: a promising material for future cancer therapy? *Nanotechnology* **21,** 85103 (2010).
2. Ferrari, M. Nanoncology. *Tumori* **94,** 197–199 (2008).
3. Manikandan, M., Hasan, N. & Wu, H. F. Platinum nanoparticles for the photothermal treatment of Neuro 2A cancer cells. *Biomaterials* **34,** 5833–5842 (2013).
4. Huang, X. & El-Sayed, M. A. Gold nanoparticles: Optical properties and implementations in cancer diagnosis and photothermal therapy. *J. Adv. Res.* **1,** 13–28 (2010).
5. Jørgensen, J. T. *et al.* Single Particle and PET-based Platform for Identifying Optimal Plasmonic Nano-Heaters for Photothermal Cancer Therapy. *Sci. Rep.* **6,** 30076 (2016).
6. Jain, P. K., Lee, K. S., El-Sayed, I. H. & El-Sayed, M. A. Calculated absorption and scattering properties of gold nanoparticles of different size, shape, and composition: Applications in biological imaging and biomedicine. *J. Phys. Chem. B* **110,** 7238–7248 (2006).
7. Loo, C., Lowery, A., Halas, N., West, J. & Drezek, R. Immunotargeted nanoshells for integrated cancer imaging and therapy. *Nano Lett.* **5,** 709–711 (2005).
8. Klingberg, H. *et al.* Uptake of gold nanoparticles in primary human endothelial cells. *Toxicol. Res.* **4,** 655–666 (2015).
9. Agilent | UV-Vis-NIR Spectroscopy Tutorial. Available at: http://www.agilent.com/en-us/products/uv-vis-uv-vis-nir/tutorial. (Accessed: 28th April 2017)
10. Martin, G. & Pretzel, B. UV-VIS-NIR spectroscopy: what is it & what does it do? - Victoria and Albert Museum. (1991). Available at: http://www.vam.ac.uk/content/journals/conservation-journal/issue-01/uv-vis-nir-spectrocopy-what-is-it-and-what-does-it-do/. (Accessed: 29th May 2017)
11. Albanese, A. *et al.* Secreted biomolecules alter the biological identity and cellular interactions of nanoparticles. *ACS Nano* **8,** 5515–5526 (2014).
12. Brun, E. & Sicard – Roselli, C. Could nanoparticle corona characterization help for biological consequence prediction? *Cancer Nanotechnol.* **5,** 7 (2014).
13. Malvern. Dynamic Light Scattering Common Terms Defined. 6 (2011). Available at: https://www.malvern.com/en/support/resource-center/Whitepapers/WP111214DLSTermsDefined.html. (Accessed: 28th April 2017)
14. Konieczny, P. *et al.* Effects triggered by platinum nanoparticles on primary keratinocytes. *Int. J. Nanomedicine* **8,** 3963–3975 (2013).
15. Stepanov AL, Golubev AN, N. S. Synthesis and Applications of Platinum Nanoparticles : A Review. *Nanotechnology* **2,** 173–199 (2013).
16. Huang, X., El-sayed, I. H., Qian, W. & El-sayed, M. A. Cancer Cell Imaging and Photothermal Therapy in the Near-Infrared Region by Using Gold Nanorods Cancer Cell Imaging and Photothermal Therapy in the Near-Infrared Region by Using Gold Nanorods. 2115–2120 (2006). doi:10.1021/ja057254a
17. Kyrsting, A., Bendix, P. M., Stamou, D. G. & Oddershede, L. B. Heat profiling of three-dimensionally optically trapped gold nanoparticles using vesicle cargo release. *Nano Lett.* **11,** 888–892 (2011).
18. Huang, X., Jain, P. K., El-Sayed, I. H. & El-Sayed, M. A. Plasmonic photothermal therapy (PPTT) using gold nanoparticles. *Lasers Med. Sci.* **23,** 217–228 (2008).
19. Wang, C. *et al.* Trifolium-like Platinum Nanoparticle-

Mediated Photothermal Therapy Inhibits Tumor Growth and Osteolysis in a Bone Metastasis Model. *Small* **11,** 2080–2086 (2015).
20. Elmore, S. Apoptosis: A Review of Programmed Cell Death. *Toxicol. Pathol.* **35,** 495–516 (2007).
21. Annexin V Conjugates for Apoptosis Detection. (2011). Available at: https://tools.thermofisher.com/content/sfs/manuals/mp13199.pdf. (Accessed: 13th May 2017)
22. Fink, S. L., Cookson, B. T., Fink, S. L. & Cookson, B. T. Eukaryotic Cells MINIREVIEW Apoptosis , Pyroptosis , and Necrosis : Mechanistic Description of Dead and Dying Eukaryotic Cells. *Infect. Immun.* **73,** 1907–1916 (2005).
23. Engeland, M. van, Nieland, Luc, J., W., Ramaekers, Frans C., S., Schutte, B. & Reutelingsperger, Chris, P., M. Annexin V-Affinity Assay: A Review on an Apoptosis Detection System Based on Phosphatidylserine Exposure. *Wiley-Liss, Inc* **31,** 1–9 (1998).
24. Vermes, I., Haanen, C., Steffens-Nakken, H. & Reutellingsperger, C. A novel assay for apoptosis Flow cytometric detection of phosphatidylserine expression on early apoptotic cells using fluorescein labelled Annexin V. *J. Immunol. Methods* **184,** 39–51 (1995).
25. Edinger, A. L. & Thompson, C. B. Death by design: Apoptosis, necrosis and autophagy. *Curr. Opin. Cell Biol.* **16,** 663–669 (2004).
26. Golstein, P. & Kroemer, G. Cell death by necrosis: towards a molecular definition. *Trends Biochem. Sci.* **32,** 37–43 (2007).
27. Proskuryakov, S. Y., Konoplyannikov, A. G. & Gabai, V. L. Necrosis: A specific form of programmed cell death? *Exp. Cell Res.* **283,** 1–16 (2003).
28. Fisher Scientific, T. LIVE/DEAD Fixable Dead Cell Stain Kits. Available at: https://tools.thermofisher.com/content/sfs/manuals/MAN0010989_LIVE_DEAD_Fixable_Dead_Cell_Stain_Kits_UG.pdf. (Accessed: 3rd May 2017)
29. Broek, B. Van De, Devoogdt, N., Hollander, A. D., Gijs, H. & Jans, K. Specific Cell Targeting with Nanobody Conjugated Branched Gold Nanoparticles for Photothermal Therapy. *ACS Nano* **5,** 4319–4328 (2011).
30. Schieber, M. & Chandel, N. S. ROS function in redox signaling and oxidative stress. *Curr. Biol.* **24,** R453–R462 (2014).
31. CellROX® Oxidative Stress Reagents. (2012). Available at: https://tools.thermofisher.com/content/sfs/manuals/mp10422.pdf. (Accessed: 3rd May 2017)
32. CellROX Deep Red Reagent, for oxidative stress detection - Thermo Fisher Scientific. Available at: https://www.thermofisher.com/order/catalog/product/C10422. (Accessed: 3rd May 2017)
33. Ormerod, M. G. *Flow Cytometry - A Basic Introduction*. (De Novo, 2008). Chapter 1-4, 7, 9.
34. Adan, A., Alizada, G., Kiraz, Y., Baran, Y. & Nalbant, A. Flow cytometry: basic principles and applications. *Crit. Rev. Biotechnol.* **37,** 163–176 (2017).
35. Brown, M. & Wittwer, C. Flow Cytometry: Principles and Clinical Applications in Hematology. *Clin. Chem.* **46,** 1221–1229 (2000).
36. Gutierrez, C. & Schiff, R. HER 2: Biology, Detection, and Clinical Implications. *Arch. Pathol.* **135,** 55–62 (2011).
37. Ravindran, A., Chandran, P. & Khan, S. S. Biofunctionalized silver nanoparticles: Advances and prospects. *Colloids Surfaces B Biointerfaces* **105,** 342–352 (2013).
38. Yamada, M., Foote, M. & Prow, T. W. Therapeutic gold, silver, and platinum nanoparticles. *Wiley Interdiscip. Rev. Nanomedicine Nanobiotechnology* **7,** 428–445 (2015).
39. Braydich-Stolle, L., Hussain, S., Schlager, J. J. & Hofmann, M. C. In vitro cytotoxicity of nanoparticles in mammalian germline stem cells. *Toxicol. Sci.* **88,** 412–419 (2005).
40. Cedervall, T. *et al.* Understanding the nanoparticle-protein corona using methods to quantify exchange rates and affinities of proteins for nanoparticles. *Proc. Natl. Acad. Sci.* **104,** 2050–2055 (2007).
41. Treuel, L., Docter, D., Maskos, M. & Stauber, R. H. Protein corona - from molecular adsorption to physiological complexity. *Beilstein J. Nanotechnol.* **6,** 857–873 (2015).
42. Cheng, X. *et al.* Protein Corona Influences Cellular Uptake of Gold Nanoparticles by Phagocytic and Nonphagocytic Cells in a Size-Dependent Manner. *ACS Appl. Mater. Interfaces* **7,** 20568–20575 (2015).
43. Mitrano, D. M. *et al.* Silver nanoparticle characterization using single particle ICP-MS (SP-ICP-MS) and asymmetrical flow field flow fractionation ICP-MS (AF4-ICP-MS). *J. Anal. At. Spectrom.* **27,** 1131 (2012).
44. Fratoddi, I., Venditti, I., Cametti, C. & Russo, M. V. How toxic are gold nanoparticles? The state-of-the-art. *Nano Res.* **8,** 1771–1799 (2015).
45. Dobrovolskaia, M. A. & McNeil, S. E. Immunological properties of engineered nanomaterials. *Nat. Nanotechnol.* **2,** 469–478 (2007).
46. Patra, H. K., Banerjee, S., Chaudhuri, U., Lahiri, P. & Dasgupta, A. K. Cell selective response to gold nanoparticles. *Nanomedicine Nanotechnology, Biol. Med.* **3,** 111–119 (2007).
47. Pan, Y. *et al.* Size-dependent cytotoxicity of gold nanoparticles. *Small* **3,** 1941–1949 (2007).
48. Zhang, X. D. *et al.* Irradiation stability and cytotoxicity of gold nanoparticles for radiotherapy. *Int. J. Nanomedicine* **4,** 165–173 (2009).
49. Takahashi, H. *et al.* Modification of gold nanorods using phosphatidylcholine to reduce cytotoxicity. *Langmuir* **22,** 2–5 (2006).
50. Villiers, C., Freitas, H., Couderc, R., Villiers, M.-B. &

Marche, P. Analysis of the toxicity of gold nano particles on the immune system: effect on dendritic cell functions. *J. Nanopart. Res.* **12,** 55–60 (2010).
51. Tedesco, S., Doyle, H., Blasco, J., Redmond, G. & Sheehan, D. Oxidative stress and toxicity of gold nanoparticles in Mytilus edulis. *Aquat. Toxicol.* **100,** 178–186 (2010).
52. Bernardi, R. J., Lowery, A. R., Thompson, P. A., Blaney, S. M. & West, J. L. Immunonanoshells for targeted photothermal ablation in medulloblastoma and glioma: An in vitro evaluation using human cell lines. *J. Neurooncol.* **86,** 165–172 (2008).
53. Hirsch, L. R. *et al.* Nanoshell-mediated near-infrared thermal therapy of tumors under magnetic resonance guidance. *Proc. Natl. Acad. Sci.* **100,** 13549–13554 (2003).
54. El-Sayed, I. H., Huang, X. & El-Sayed, M. A. Selective laser photo-thermal therapy of epithelial carcinoma using anti-EGFR antibody conjugated gold nanoparticles. *Cancer Lett.* **239,** 129–135 (2006).